Radiation dose risk variability and its implication in industrial and mining regions, NW Nigeria

Ologe Oluwatoyin[1, *], Joseph Aisabokhae[2]

Dept. of Applied Geophysics, Federal University Birnin Kebbi, Birnin Kebbi, Kebbi State, Nigeria.

**Corresponding author: oluwatoyin.ologe@fubk.edu.ng*

Abstract

The study area in the southern part of Kebbi State, Northwestern Nigeria, has witnessed intense mining activities and upscale industrialization in recent years. These events have necessitated deeper and insightful studies into radiological hazard evaluation to mitigate associated adverse consequences and enforce environmental protective measures. A total of 45 sampled locations each were taken for industrial and mining sites in Northwestern Nigeria to determine the concentration of Potassium-40, Thorium-232 and Uranium-238 radionuclides as applied to radiological hazard analysis. The mean value of the absorbed dose in the industrial site was 90 nGy/h, whereas the mining site recorded a mean value of 210 nGy/h. Other radiological indices such as radium equivalent factor, external risk assessment, internal index and representative gamma index recorded mean values of 187.68, 0.507, 0.547 and 0.768 respectively, whereas the same hazard indices presented higher values of 412.58, 1.114, 1.231 and 1.675 respectively in the mining site. The variability studies showed that the dose risk ratio of the industrial region to the mining region is 1:2. The mining site presented radiological hazard indices higher than the acceptable global threshold, hence should be classified as a restricted zone to forestall health-related crises which may manifest among local dwellers.

Keywords: Dose risk; industrial site; mining site; Northwestern Nigeria; radiological hazards.

1. Introduction

The study area lies between latitude 11°24' to 11°30' north and longitude 5°8' to 5°16' East as shown in Figure 1. The region is dominated by plutonic emplacements which have given clues to mineral exploration and also provided raw materials for construction and industrialization (Aisabokhae & Oresajo, 2019; Aisabokhae & Tampul, 2020). The environment is continually threatened by natural and anthropogenic causes which can affect the environment's safety for human habitation (Horasan & Arik, 2019; Ozturk & Arici, 2021). Various characteristics of in-situ elements in rocks or soils make them useful to the environment. However, a major characteristic of concern is the natural radioactivity potential of elements in rocks and soils.

Natural radionuclides can be categorized into cosmogonic, primordial and anthropogenic (UNSCEAR, 2000). Primordial and cosmogonic radionuclides like potassium (^{40}K) and the nuclides from thorium (^{232}Th) and uranium (^{238}U) series, and their decay products exist in all ground formations at the trace level. Their ubiquitous nature in the environment makes them a major source of radiation for the human population. ^{40}K, ^{232}Th and ^{238}U are the three major radionuclides whose radioactive concentrations are often monitored in the environment to

control or mitigate the adverse effects which their enrichment may portend to human population. The knowledge of the rate of exposure of man to radiation is important in determining the degree of threat to human life which the environment poses.

In this study, a comparative analysis is being presented to inform the research community of the contrast between the radiological significance of measured radiation doses in mining and in industrial sites. The consequences of continuous human exposure to background ionizing radiation can result in major health challenges including stunted growth, skin diseases and cancer (Kumari *et al*., 2017). As such, geological and geographical locations with sizeable population density such as the mining and industrial sites studied in this work must be assessed for their environmental radioactivity indices.

2. Geological setting of the study area

The Precambrian basement complex (Figure. 1) in Northern Nigeria is a mobile belt which is dominated by Neoproterozoic rocks due to the ubiquitous nature of the Pan-African event that occurred around 600 Ma (Kogbe, 1979). The region is primarily dominated by migmatite gneiss of granodiorite-to-granite composition (Ramadan & Abdel Fattah, 2010).

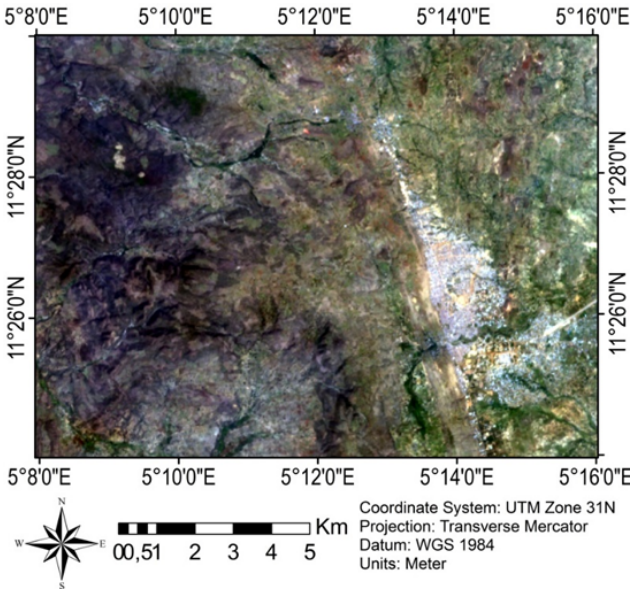

Fig. 1. Landsat-8 false colour image of the study region showing lineation trend and the exposed basement rock emplaced in the area (USGS, 2015).

3. Materials and methods

3.1 Data acquisition

In the area under study, 377 sites were earmarked for radioactivity concentration measurement encompassing mining and industrial sites. 23 more sites are expected to be delineated from satellite images depicted as alteration zones for potential future mining activities using ERDAS imaging software, thus bringing the total proposed sample site to 400 throughout the region.

The Scintrex GAD-6 model portable gamma-ray spectrometer was used to conduct ground surface spectrometric survey. The four-channel digital spectrometer is designed with

Scintrex gamma-ray sensors (KEL, 1978). The measurement of radioelement concentration can be effectively performed by using a portable detector placed on a rock surface to detect radiation from approximately 0.15 m depth and 1.0 m radius with minimal contribution from deep sources (McCay *et al*., 2014; Lovborg, 1984). The energy peaks were given as 1.76 MeV from 214Bi (uranium) and 2.61 MeV from 208Ti (thorium) while potassium measurement was directly from 1.46 MeV emitted from ^{40}K. The spectrometer used in this study was calibrated using laboratory-grade concrete calibration pads of plain potassium, thorium and uranium of the Canadian model (Killeen & Conaway, 1978). The measurements were taken five (5) times in each sample point with the geographical coordinate, elevation and site number properly recorded from the GPS device. While recording the measured data, the prevalent geographic features and geologic imprints of the area were observed.

3.2 Data processing

The measured primordial radioactive concentration data were computed for the statistical mean, standard deviation and covalence of variance and then used as input data to calculate the following parameters:

Radium equivalent radiological factor (Ra_{eq})

This radiological activity refers to the central factor in comparing the radionuclides in any material. In the study area, the concentration of the radioelement emanating from the surface can be examined using the radium equivalent factor. For each of the radioelements that produce gamma dose, equation (1) (Joel *et al.,* 2020) will estimate the radiological factor as follows:

$$Ra_{eq} = C_U + 1.43\ C_{Th} + 0.077\ C_K \quad (1)$$

External risk assessment (H_{ex})

The external risk assessment (H_{ex}) activity associated with gamma radiation emanating from the earth's surface can be examined using equation (2) (Joel *et al*., 2020) thus:

$$H_{ex} = C_U/370 + C_{Th}/259 + C_K/4810 \quad (2)$$

C_K, C_{Th}, and C_U are the activity concentration in Bq/kg.

Internal hazard index (H_{in})

The determination of the internal hazard represented by H_{in} can be examined using equation (3) (Joel *et al*., 2020) thus:

$$H_{in} = (C_U/185) + (C_{Th}/259) + (C_K/4810) \quad (3)$$

Such that C_U, C_{Th}, and C_K are activity concentrations of 238-U, 232-Th, and 40-K, respectively.

Representative gamma index (Iγ)

Representative gamma index represents the hazard associated with occurring primordial radioactive concentration in an area under investigation. The representative index (Iγ) activity is estimated by the use of equation (4) (Joel *et al*., 2020) thus:

$$I\gamma = C_U/300\ (Bqkg^{-1}) + C_{Th}/200\ (Bqkg^{-1}) + C_K/3000\ (Bqkg^{-1}) \quad (4)$$

Representative alpha index (Iα)

Representative alpha index (Iα) is an important radiological index activity that can examine the measure of protection for the human population subjected to radiation exposure due to proximity to gamma-ray sources. The evaluation of Iα is performed using equation (5) (Joel *et al*., 2020) thus:

$$I\alpha = C_U/200\ (Bqkg^{-1}) \quad (5)$$

Annual effective dose (AED)

The AED for the measured locations can be assessed by applying equation (6) (Joel *et al*., 2020).

$$AED = (0.49C_U + 0.76C_{Th} + 0.048C_K) \times 87.6 \times 10^{-2} \quad (6)$$

Excess lifetime cancer risk (ELCR)

A major radiological parameter to be calculated in this study is the excess lifetime cancer risk (ELCR), which can be calculated using equation (7) (Taskin *et al*., 2009).

$$ELCR = AED \times LD \times RF \quad (7)$$

Given that AED is the annual effective dose, Life Duration (LD) is estimated at 70 years, and the risk factor is determined as 0.05 Svy^{-1} (Taskin *et al*., 2009).

Dose risk

The computation for dose risk is given by equation (8) (Durham, 2007; Martin, 2011).

$$G = fHP \quad (8)$$

Such that G represents the number of potential casualties likely to die from radiation-related complications. F is the dose risk conversion factor (DRCF) of 5% per Sievert (ICRP, 1991). H is the estimated annual effective dose, whereas P is the total number of dwellers in the sampling area.

4. Results and discussion

Radioactive concentration measurement from 45 locations each in both the mining and industrial sites were collected to serve as input data for this study. The absorbed dose activity computed in the industrial and mining sites is presented in Table 1. In the industrial site, the absorbed dose ranged from 71 to 125 nGy/h with an estimated average of 96 nGy/h. In the mining site, the gamma absorbed dose values ranged from 152 to 249 nGy/h with an estimated mean value of 210 nGy/h.

Some radiological hazard indices such as radium equivalent factor, external risk assessment, internal hazard index and representative gamma index estimated within the industrial site and mining site are shown in Table 2. The radium equivalent factor, which compares the radionuclide content present in a material, ranged from 140 to 247 with a mean value of 187 in the industrial site, whereas the radium equivalent factor in the mining site

ranged from 301 to 496 with an average of 412 in the area. For building materials to be considered acceptable, the value of Ra_{eq} must be below unity for the induced radiation from natural radioactivity. This corresponds to 370 Bq/kg (Samwell, 2010).

Table 1. Absorbed dose computation.

Site No	Absorbed Dose D (nGy/h)							
	Industrial Site				Mining site			
	0.0414 K	0.621 Th	0.462 U	Total	0.0414 K	0.621 Th	0.462 U	Total
1	70.415	11.638	4.399	86.452	122.338	20.362	12.604	155.304
2	67.538	10.436	5.512	83.485	117.129	27.156	12.992	157.278
3	76.233	12.601	5.215	94.049	118.490	28.268	11.999	158.757
4	61.409	12.637	6.510	80.556	138.679	41.901	12.256	192.835
5	62.420	12.939	7.269	82.628	150.458	37.068	11.491	199.017
6	68.380	14.275	6.242	88.898	173.173	27.056	13.928	214.157
7	72.579	12.957	7.503	93.039	142.786	33.820	16.392	192.999
8	77.918	11.194	7.880	96.992	157.040	23.243	12.490	192.774
9	74.885	12.377	6.624	93.887	176.400	37.068	12.233	225.701
10	53.297	12.430	7.081	72.808	167.381	27.076	11.491	205.948
11	65.193	12.400	5.717	83.309	129.245	28.278	15.999	173.522
12	52.001	14.969	6.316	73.286	167.226	40.370	16.084	223.680
13	53.271	12.614	8.633	74.518	168.897	36.087	15.822	220.806
14	51.968	14.291	5.244	71.522	182.27	27.012	12.604	221.887
15	65.983	13.085	5.129	84.198	182.439	28.248	13.329	224.015
16	66.864	11.754	4.656	83.274	172.590	51.819	15.805	240.215
17	71.179	11.820	10.395	93.395	173.199	46.938	10.949	231.087
18	64.817	12.369	4.587	81.774	176.841	43.870	11.092	231.802
19	80.224	12.503	5.135	97.862	169.380	62.101	9.323	240.814
20	92.133	12.389	5.592	110.114	170.323	47.427	28.449	246.199
21	82.207	15.468	4.650	102.325	153.969	41.888	23.582	219.439
22	79.758	16.537	5.575	101.869	168.470	29.068	26.155	223.692
23	85.770	15.455	9.191	110.418	143.020	37.080	27.889	207.989
24	80.185	17.639	9.813	107.638	169.027	37.852	27.918	234.796
25	88.906	16.794	10.966	116.667	167.783	56.020	25.670	249.473
26	72.747	15.887	3.857	92.491	125.811	51.711	20.649	198.171
27	77.490	16.164	4.639	98.293	162.496	41.964	20.472	224.932
28	72.565	16.797	5.021	94.384	182.957	36.231	21.202	240.390
29	79.421	21.794	5.169	106.384	173.264	46.550	20.204	240.018
30	79.537	19.431	5.226	104.195	116.663	25.513	21.619	163.794
31	86.418	23.740	5.689	115.847	170.776	24.302	22.766	217.844
32	84.397	20.513	5.763	110.673	139.651	28.286	24.848	192.785
33	84.228	10.584	6.065	100.878	149.913	15.740	25.778	191.432
34	82.997	11.134	6.225	100.356	176.517	23.455	27.564	227.536
35	80.639	15.581	8.365	104.585	155.291	29.544	25.168	210.003
36	80.211	15.554	5.780	101.545	154.086	22.747	28.432	205.264
37	84.099	15.707	5.215	105.021	165.204	38.096	29.293	232.593
38	53.556	16.966	15.999	86.521	175.104	41.976	23.958	241.039
39	58.182	20.084	12.233	90.500	170.958	49.760	22.743	243.460
40	54.411	19.237	9.928	83.577	162.405	28.783	25.967	217.155
41	61.318	23.047	12.627	96.992	147.322	47.009	26.298	220.628
42	92.146	22.616	10.949	125.710	103.808	25.263	23.439	152.510
43	79.537	24.320	5.831	109.689	127.431	25.127	21.562	174.120
44	84.397	19.454	6.356	110.207	118.153	33.820	28.603	180.576
45	96.344	18.151	5.831	120.326	128.766	40.355	28.466	197.587
Mean	73.560	15.563	6.947	96.070	154.781	35.407	19.946	210.134

Table 2. Deduced radium equivalent, external and internal risk indices, and gamma index.

Site	Industrial site				Mining site			
	Ra_{eq}	H_{ex}	H_{in}	I_y	Ra_{eq}	H_{ex}	H_{in}	I_y
1	167.286	0.452	0.477	0.692	301.706	0.815	0.888	1.240
2	161.574	0.436	0.468	0.668	308.504	0.833	0.909	1.255
3	182.092	0.492	0.522	0.753	311.446	0.841	0.911	1.268
4	157.405	0.425	0.463	0.643	380.944	1.029	1.100	1.542
5	161.624	0.436	0.478	0.660	390.067	1.053	1.120	1.593
6	173.564	0.469	0.505	0.711	414.534	1.119	1.201	1.713
7	181.065	0.489	0.533	0.743	378.929	1.023	1.120	1.540
8	187.751	0.507	0.553	0.774	372.638	1.006	1.080	1.542
9	182.119	0.491	0.531	0.750	439.922	1.188	1.259	1.807
10	143.076	0.386	0.427	0.580	398.534	1.076	1.143	1.649
11	162.180	0.438	0.471	0.666	340.130	0.918	1.012	1.384
12	144.857	0.391	0.428	0.585	438.801	1.185	1.279	1.788
13	146.811	0.396	0.447	0.593	431.478	1.165	1.257	1.765
14	140.950	0.381	0.411	0.571	428.489	1.157	1.230	1.776
15	163.957	0.443	0.472	0.674	433.216	1.170	1.248	1.793
16	161.506	0.436	0.463	0.667	474.538	1.281	1.374	1.921
17	182.106	0.492	0.552	0.743	453.921	1.226	1.290	1.851
18	158.965	0.429	0.456	0.655	453.935	1.226	1.291	1.857
19	189.116	0.511	0.541	0.784	478.231	1.291	1.346	1.931
20	211.991	0.572	0.605	0.882	487.573	1.317	1.483	1.958
21	198.580	0.536	0.563	0.820	433.868	1.172	1.309	1.747
22	198.489	0.536	0.569	0.816	436.884	1.180	1.333	1.779
23	215.013	0.581	0.635	0.881	411.756	1.112	1.275	1.651
24	210.997	0.570	0.628	0.858	461.965	1.247	1.411	1.867
25	227.767	0.615	0.678	0.930	496.622	1.341	1.491	1.987
26	180.234	0.487	0.509	0.741	397.769	1.074	1.196	1.578
27	191.386	0.517	0.543	0.788	443.170	1.197	1.317	1.794
28	184.512	0.498	0.527	0.756	469.604	1.268	1.392	1.918
29	209.090	0.565	0.595	0.852	473.178	1.277	1.395	1.916
30	203.990	0.551	0.581	0.835	322.524	0.871	1.000	1.301
31	227.710	0.615	0.649	0.928	422.866	1.142	1.275	1.735
32	216.680	0.585	0.619	0.886	378.656	1.023	1.168	1.531
33	194.157	0.524	0.560	0.807	370.867	1.001	1.153	1.520
34	193.479	0.522	0.559	0.803	441.978	1.194	1.355	1.809
35	203.966	0.551	0.600	0.835	411.335	1.111	1.258	1.670
36	197.512	0.533	0.568	0.813	400.505	1.082	1.248	1.629
37	203.874	0.550	0.581	0.841	458.394	1.238	1.409	1.848
38	173.306	0.468	0.561	0.683	474.196	1.280	1.420	1.921
39	180.941	0.489	0.560	0.718	481.775	1.301	1.434	1.941
40	166.988	0.451	0.509	0.665	424.542	1.146	1.299	1.727
41	194.447	0.525	0.601	0.770	439.174	1.186	1.339	1.754
42	247.130	0.667	0.732	1.003	301.981	0.815	0.952	1.208
43	216.557	0.585	0.618	0.878	341.540	0.922	1.048	1.384
44	215.525	0.582	0.619	0.882	359.542	0.971	1.138	1.430
45	233.609	0.631	0.665	0.964	394.033	1.064	1.231	1.567
Mean	187.687	0.507	0.547	0.768	412.584	1.114	1.231	1.675

The internal hazard index estimated in the industrial site ranged from 0.411 to 0.678 with a mean value of 0.547, whereas the values recorded in the mining site ranged from 0.888 to 1.491 with an average estimate of 1.231. The representative gamma index estimated in the industrial site ranged from 0.571 to 1.003 with an estimated average of 0.768, whereas the gamma index estimated in the mining site ranged from 1.208 to 1.987 with an average value of 1.675.

Table 3. Deduced alpha index, annual effective dose and excess cancer lifetime risk indices.

Site	Industrial site			Mining site		
	I_α	AED	ELCR	I_α	AED	ELCR
1	0.048	0.106	0.372	0.136	0.190	0.667
2	0.060	0.102	0.358	0.141	0.193	0.675
3	0.056	0.115	0.404	0.130	0.195	0.681
4	0.070	0.099	0.346	0.133	0.236	0.828
5	0.079	0.101	0.355	0.124	0.244	0.854
6	0.068	0.109	0.382	0.151	0.263	0.919
7	0.081	0.114	0.400	0.177	0.237	0.828
8	0.085	0.119	0.416	0.135	0.236	0.827
9	0.072	0.115	0.403	0.132	0.277	0.969
10	0.077	0.089	0.313	0.124	0.253	0.884
11	0.062	0.102	0.358	0.173	0.213	0.745
12	0.068	0.090	0.315	0.174	0.274	0.960
13	0.093	0.091	0.320	0.171	0.271	0.948
14	0.057	0.088	0.307	0.136	0.272	0.952
15	0.056	0.103	0.361	0.144	0.275	0.962
16	0.050	0.102	0.357	0.171	0.295	1.031
17	0.113	0.115	0.401	0.119	0.283	0.992
18	0.050	0.100	0.351	0.120	0.284	0.995
19	0.056	0.120	0.420	0.101	0.295	1.034
20	0.061	0.135	0.473	0.308	0.302	1.057
21	0.050	0.125	0.439	0.255	0.269	0.942
22	0.060	0.125	0.437	0.283	0.274	0.960
23	0.099	0.135	0.474	0.302	0.255	0.893
24	0.106	0.132	0.462	0.302	0.288	1.008
25	0.119	0.143	0.501	0.278	0.306	1.071
26	0.042	0.113	0.397	0.223	0.243	0.851
27	0.050	0.121	0.422	0.222	0.276	0.965
28	0.054	0.116	0.405	0.229	0.295	1.032
29	0.056	0.130	0.457	0.219	0.294	1.030
30	0.057	0.128	0.447	0.234	0.201	0.703
31	0.062	0.142	0.497	0.246	0.267	0.935
32	0.062	0.136	0.475	0.269	0.236	0.828
33	0.066	0.124	0.433	0.279	0.235	0.822
34	0.067	0.123	0.431	0.298	0.279	0.977
35	0.091	0.128	0.449	0.272	0.258	0.901
36	0.063	0.125	0.436	0.308	0.252	0.881
37	0.056	0.129	0.451	0.317	0.285	0.998
38	0.173	0.106	0.371	0.259	0.296	1.035
39	0.132	0.111	0.388	0.246	0.299	1.045
40	0.107	0.102	0.359	0.281	0.266	0.932
41	0.136	0.119	0.416	0.285	0.271	0.947
42	0.118	0.154	0.540	0.254	0.187	0.655
43	0.063	0.135	0.471	0.233	0.214	0.747
44	0.069	0.135	0.473	0.310	0.221	0.775
45	0.063	0.148	0.516	0.308	0.242	0.848
Mean	0.075	0.118	0.412	0.216	0.258	0.902

Other hazard indices comprising alpha index, annual effective dose and excess cancer lifetime risk indices have been computed in Table 3. Within the industrial site, the alpha index showed varying indices ranging from 0.042 to 0.173 with a mean value of 0.075, whereas a range of values from 0.101 to 0.317 and a mean value of 0.216 was recorded in the mining site. The annual effective dose in the industrial site presented values ranging from 0.088 to 0.154 with

an average of 0.118, whereas the mining site showed values ranging from 0.187 to 0.306 and had an average of 0.258 in the area. The excess cancer lifetime risk indices produced in the area reflected varying indices for the industrial and mining sites. ELCR indices in the industrial site ranged from 0.307 to 0.540 with an average of 0.412, whereas in the mining site, it ranged from 0.655 to 1.071 with an average of 0.902. The ELCR values in both industrial and mining sites are below the recommended safe limit of 3.75 X 10^{-3} (UNSCEAR, 2000). The result of ELCR in the industrial site is comparable to the values obtained in soil samples collected at Covenant University, Ota, Nigeria (Joel *et al*., 2020). More so, the results of some radiological hazards deduced in the mining site are similar to those obtained in a kaolin mining field in Ifonyintedo, Nigeria (Adagunodo *et al*., 2018).

The estimated dose risk from primordial radiation sources was deduced for industrial and mining sites in the region. The dose risk indices may be suitable for estimating possible adverse implications due to gamma-ray exposures. The AED disparity between the industrial site and mining site is displayed in Figure 2. All AED estimations in the mining site are numerically higher than those obtained in the industrial site. In Figure 3, the ELCR activity in the mining site also appears to be higher than in the industrial site.

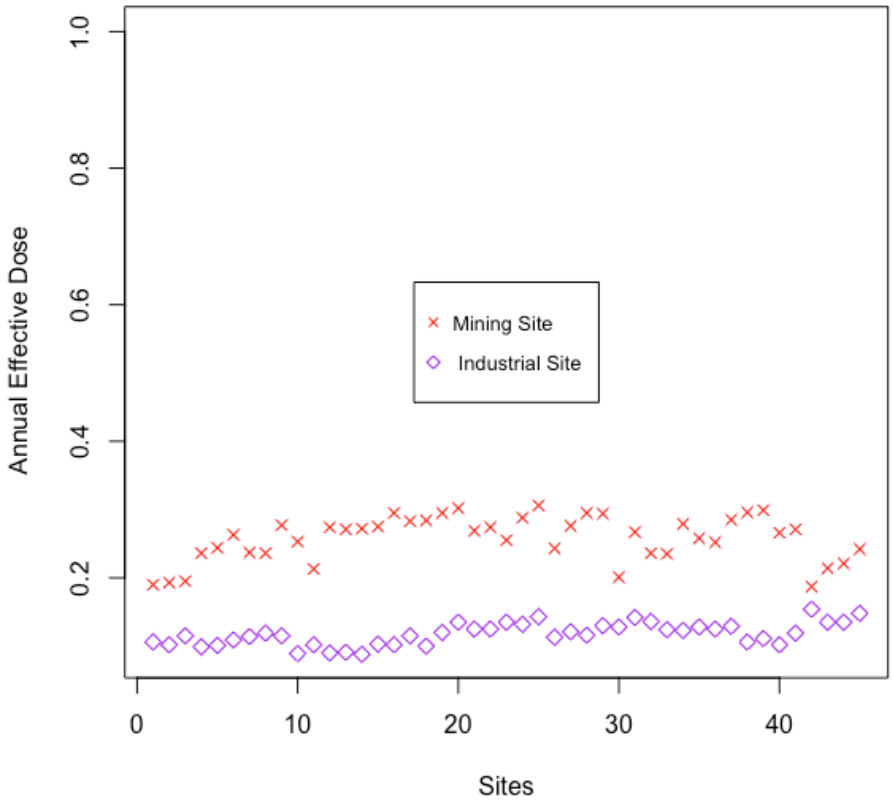

Fig. 2. Plot of AED variability in industrial and mining sites.

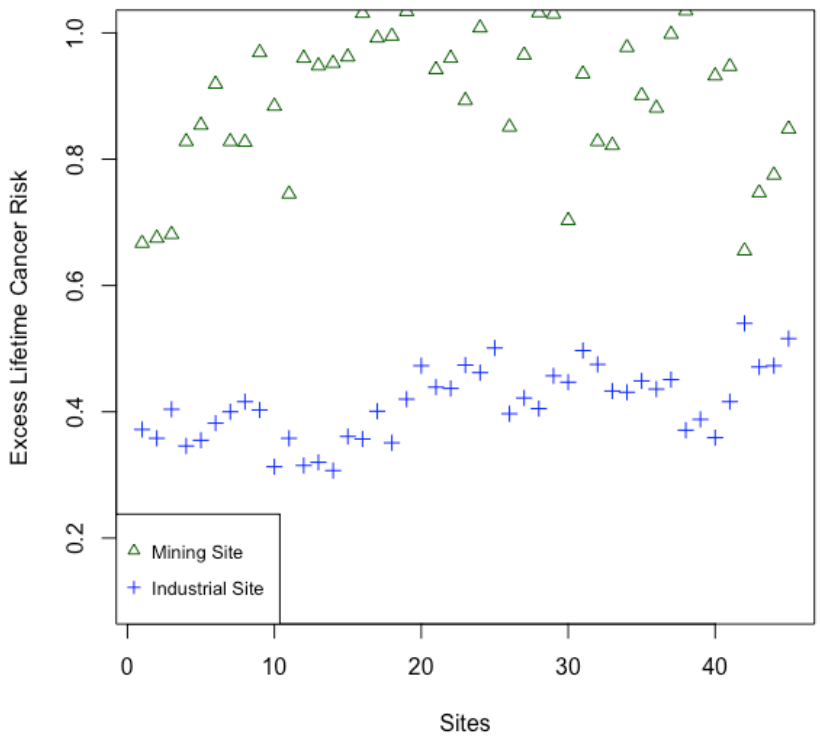

Fig. 3. Plot of ELCR variability between industrial and mining sites.

With an estimated population of 14,272 dwellers in the industrial area, and a dwindling 3,414 inhabitants in the mining area (NBS, 2016), a credible dose risk analysis may provide information about the possibility of fatal cancer occurrence in the area. Table 4 provides a comparative analysis of the dose risk in the industrial and mining sites.

Table 4. Dose risk computation

Site	AED (mean)	DRCF (5% Sv^{-1})	Dose risk per year
Industrial	0.118	0.05	84
Mining	0.258	0.05	44

Predictions from the comparative analysis suggest that 84 people (0.6%) of the entire population living in the industrial sites may die due to exposure to gamma-ray radiation, whereas 44 people (1.3%) are in danger of becoming casualties of exposure to gamma-ray radiation in the mining site (Table 4). Regarding DRCF indices, certain parameters such as age, gender, personal habits, diet, etc., may influence the degree of intensity.

5. Conclusion

The results of the predicted radiation dose risk in the study area were presented based on the measurements of primordial radioactive concentrations. Some conclusions drawn from the study are listed.

i. The Ra_{eq} activity estimated in the industrial site is averaged at 187.68 Bq/kg. It is well below the recommended limit of 370 Bq/kg as stated by UNSCEAR (2000), whereas in the mining site, the Ra_{eq} presented an average of 412 Bq/kg which is well above the recommended limit.

ii. The mean annual effective dose in the industrial site showed 0.118 mSv/y, whereas the mean value obtained from the mining site was 0.258 mSv/y. The AED activity in both sites was below the global limit of 0.70 mSv/y (UNSCEAR, 2000).

It is recommended that the mining site be restricted from residual inhabitation for health safety purposes.

ACKNOWLEDGEMENTS

The authors wish to thankfully acknowledge the proofreaders and editors in the Department of Language and Linguistics, Nasarawa State University, Keffi for providing language editing service in support of this manuscript.

References

Adagunodo, T.A., George, A.I., Ojoawo, I.A., Ojesanmi K., & Ravsankar, R. (2018). Radioactivity and radiological hazards from a Kaolin field in Ifonyintedo, Nigeria. MethodX, **5**: 362-314.

Aisabokhae, J.E., & Oresajo B. (2019). The magnetic response of hydrothermal alteration in iron-oxide basement complex, NW Nigeria. Geology, Geophysics and Environment, **45**(2): 145–156. http://dx.doi.org/10.7494/geol.2019.45.2.145.

Aisabokhae, J., & Tampul H. (2020). Statistical variability of radiation exposures from Precambrian basement rocks, NW Nigeria: Implication on radiogenic heat production. Scientific African, **10**: 1-11. https://doi.org/10.1016/j.sciaf.2020.e00577

Durham, J. (2007). Concepts, quantities, and dose limits in radiation protection dosimetry. Radiation Measurement, **41**:28-35.

Horasan, B.Y., & Arık, F. (2019). Assessing Heavy Metal Pollution in the surface soils of Central Anatolia Region of Turkey, Carpathian Journal of Earth and Environmental Sciences, **14**(1): 107–118.

ICRP (1991). Annual limits on intake of radionuclides by workers based on 1990 recommendations. International Commission of Radiological Protection. Annals of the ICRP 21, Publication 4.

Joel, E.S., Omeje, D.K, Adewoyin, O., Olawole, O.C., Akinwumi, A., Erubami, S., & Adeyemi, G.A. (2020). Assessment of background radionuclide and gamma dose rate distribution in urban-setting and its radiological significance. Sci. Afri. **8**:1-8.

Kelvin Energy Limited (1978). Report on airborne electromagnetic, magnetometer and radiometric survey. Kettle River Area, British Columbia. Appendix III, gad-6 and gsa-42 specifications.

Killeen, P.G., & Conaway, J.G. (1978). New facilities for calibrating gamma-ray spectrometric logging and surface exploration equipment. CIM Bull **71**:84–87.

Kogbe, C. (1979). Geology of the south-eastern sector of the Iullemmeden Basin. Bulletin of Department of Geology, Ahmadu Bello University, Zaria, **2**(1):34–78.

Kumari, R., Kant, K., & Garg, M. (2017). Natural radioactivity in rock samples of Aravali hills in India. Int. J. Radiat. Res. **15**:91-398.

Lovborg, L. (1984). The calibration of portable and airborne gamma-ray spectrometers theory, problems, and facilities. Rise Natl. Lab 2456. pp. 3–207

Martin, M. M. (2011). Measurements of the elemental and radionuclide concentrations of environmental and geological samples from selected areas of Kibwezi District, Kenya. Msc. Thesis (Physics), Kenyatta University, Kenya.

McCay, A.T., Harley, T.L., Younger, P.L., Sanderson, D.C., & Cresswell, A.J. (2014). Gamma-ray spectrometry in geothermal exploration: state of the art techniques. Energies **7**:4757–4780. https://doi.org/10.3390/en7084757

Nigeria Bureau of Statistics (2016). National population estimates. Population forecast publication.

Ozturk, A., & Arici, O.K. (2021). Carcinogenic-potential ecological risk assessment of soils and wheat in the eastern region of Konya (Turkey). Environ Sci Pollut Research, **28**:15471–15484.

Ramadan T.M., & Abdel Fattah M.F. (2010). Characteristics of gold mineralization in Garin Hawal area, Kebbi State, NW Nigeria, using remote sensing. The Egyptian Journal of Remote Sensing and Space Science, **13**:153–163. https://doi.org/10.1016/j.ejrs.2009.08.001.

Samwell, O. (2010). Radiometric survey and estimation of radiation exposure from Archean rocks: A case study of Migori gold belt company, Kenya. M.Sc. Dissertation, School of Pure and Applied Sciences, Kenyatta University, Kenya.

Taskin, H., Karavus, M., Ay, P. *et al.* (2009). Radionuclide concentrations in soils and life time cancer risk due to gamma radioactivity in Kirklareli, Turkey. J. of Environ. Radioat. **100**:49-53. https://doi:10.1016/j.jenvrad.2008.10.012

United States Geological Survey (2015). Landsat-8 (L8) data user handbook. Version 1.0

UNSCEAR (2000). Sources and effects of ionizing radiation. Report of the United Nations Scientific Committee on the Effects of Ionizing Radiation to the General Assembly. United Nations, New York.

Submitted: 15/07/2022
Revised: 19/10/2022
Accepted: 30/10/2022
DOI: 10.48129/kjs.15207